

Negative-ion formation in collisions of low-energy electrons with neutral sodium clusters

V. Kasperovich, G. Tikhonov, K. Wong, and V. V. Kresin

Department of Physics and Astronomy, University of Southern California, Los Angeles, California 90089-0484

(Received 3 April 2000; published 7 November 2000)

Electron collisions with neutral sodium clusters in the 0–3 eV energy range have been studied in a crossed-beam geometry, and direct evidence for the formation of Na_n^- anions has been obtained. The dependence of ion formation efficiency on the electron energy is well represented by the Langevin cross section, suggesting that the electrons are captured by the polarization field of the cluster. This is consistent with the highly polarizable nature of alkali-metal clusters.

PACS number(s): 36.40.Wa, 34.80.Ht

I. INTRODUCTION

Free-electron attachment to molecules is a venerable topic that has received much experimental and theoretical attention in the literature (see, e.g., the recent reviews [1–4] and references therein). In addition to its obvious importance in the fields of spectroscopy and mass spectrometry, low-energy electron attachment has been invoked in such diverse contexts as plasma discharges, combustion, excimer laser operation, explosives detection [2], and DNA radiation damage [5].

In the cluster domain, on the other hand, this subject has been explored to a considerably lesser degree. Most of the studies up to date have dealt with molecular clusters [3,4,6–12] and fullerenes [3,13–18], but only very few with metal clusters [19].

Alkali-metal nanoclusters are noted for being highly polarizable [20–22]. The strength of their long-range interactions with charged and neutral particles (for a review, see Refs. [23,24]) is a direct manifestation of the high cluster polarizability. Recent studies of low-energy inelastic electron collisions with sodium clusters [25,26] found that in the 1–5 eV electron energy range the inelastic integral cross section exceeded the geometrical cluster cross section by a factor of ~ 2 –3. For $E \leq 1$ eV it was found that the enhancement was even more dramatic, with cross sections rising strongly as $E \rightarrow 0$. It was conjectured that this behavior was due to efficient negative-ion formation. Indeed, the experimentally measured integral cross sections in this energy range were quite well represented by the Langevin expression for electron capture in the polarization field of a polarizable target [23,27–29]. An incoming slow electron polarizes the neutral cluster and is attracted by the resulting dipole field. For impact parameters below a certain critical value, the electron spirals into the center of force and is captured. If the target were a classical perfectly conducting sphere, this would represent the electron's attraction to its own image charge. For real clusters, one uses the experimentally measured dipole polarizability α .

It is important to note that, while the description above is classical, the quantum-mechanical capture cross section is practically identical to the Langevin value in the energy region of interest. Indeed, the exact solution [30] descends to the classical value and oscillates about it by no more than a few percent when the electron collision energy E satisfies

$(8\alpha E)^{1/4} > 1$, where E and α are expressed in atomic units. In view of the high polarizability of metal clusters (e.g., for Na_n , $\alpha_n \approx 64n$ a.u.; see Sec. III), for $n \geq 10$ this inequality is already satisfied at energies in the meV range, in contrast to the typical situation in atomic and molecular scattering [2]. This justifies the use of the term ‘‘Langevin capture’’ even in the sub-eV range where the de Broglie wavelength of the incident electron exceeds the radius of the cluster.

The calculation predicts that the integral polarization capture cross section should be inversely proportional to the velocity of the incoming electron, i.e., to the square root of the collision energy. The beam depletion technique employed in our previous work [25,26] was well suited for measuring absolute cross sections, but could not capture the reaction products. The evidence for the existence of efficient electron capture was therefore compelling, but indirect.

The present experiment was designed to provide direct evidence for negative-ion formation at low electron impact energies, and to verify that this anion yield indeed follows the Langevin mechanism. The rest of the paper is organized as follows. Sec. II gives a detailed description of data acquisition and analysis. In Section III our main results are presented and compared with the predictions of the polarization picture. Section IV contains the summary.

II. EXPERIMENT

The basic scheme of the experiment was to pass a collimated supersonic beam of neutral metal clusters through the collision region of a low-energy high-current electron gun, to extract the resulting negative cluster ions, and to monitor the efficiency of anion formation as a function of electron energy. The experimental setup builds upon that used for the measurement of e^- - Na_n interaction cross sections described in Ref. [26], where further details about the cluster beam and electron gun construction can be found. The arrangement was modified to incorporate a channel electron multiplier (also referred to as a CEM, or a Channeltron; Detector Technology, Palmer, MA) mounted on a movable XYZ stage and facing the downstream aperture of the electron gun (Fig. 1). The design allowed neutral particles to fly freely through the Channeltron and be detected further downstream in the manner described in detail previously (photoionized by UV light from an arc lamp, passed through a quadrupole mass analyzer, and detected by an ion counter). In this way, we could

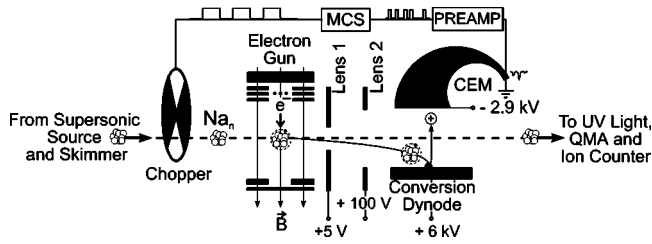


FIG. 1. Section of experimental setup used for negative-ion detection (not to scale). A beam of neutral sodium clusters is generated in a supersonic expansion source ($T_{source} = 880$ K, $T_{nozzle} = 1030$ K, Ar carrier gas pressure 8 bar). A cluster captures an electron in the scattering region of the electron gun and becomes a negative ion. It is extracted by ion optics and accelerated toward a stainless steel conversion dynode, producing positive fragments that are subsequently detected by the Channeltron and result in a TTL pulse registered by a multichannel scaler board. The conversion dynode and Channeltron are located approximately 10 mm from the collision region. Neutral clusters remaining in the beam continue freely through the negative-particle detector toward the beam detector, where they are ionized by filtered UV light, mass analyzed by a quadrupole mass analyzer (QMA), and registered by an ion counter.

monitor the sodium cluster mass spectrum simultaneously with the anion counts.

The role of the Channeltron was to detect any negatively charged particle exiting the scattering region of the electron gun, where electron and cluster beams crossed each other. At the present stage of the experiment we are not able to mass select anions before feeding them into the CEM detector. Normally, the direct detection efficiency of a commercial Channeltron drops as $m^{-1/2}$, where m is the mass of the incoming particle of a given energy [31,32]. To boost the detection efficiency of heavy ions and make it more uniform, a conversion dynode is one of the most commonly used options [32–34]. Thus we chose a CEM detector unit containing a built-in conversion dynode with an off-axis Channeltron overlooking it, as indicated in Fig. 1. The dynode was biased by a high positive voltage of up to 6 kV. The Channeltron cone was floated at -2.9 kV and the channel exit was grounded, providing a voltage gradient across the channel required to create a detectable electron avalanche. In this detection mode, an incoming negative ion is attracted by the positively charged conversion dynode, hits it, and breaks up into pieces, some of which are positively charged [35]. The positive fragments are accelerated toward the Channeltron entrance by the potential difference of about 9 kV, where secondary electrons are ejected upon impact and an electron avalanche is created. Finally, an all-in-one preamplifier and discriminator unit (Advanced Scientific Instruments Corp., Wheat Ridge, CO) is used to convert the small negative CEM output pulse into a logic (TTL) pulse 100 nsec wide.

This detection technique is beneficial in two ways. First, the negative cone voltage allows the Channeltron exit to be grounded, which allows for an easy connection to pulse counting electronics. Secondly, the high negative voltage at the CEM cone repels stray electrons that are produced in large quantities at the electron gun cathode. While a stray electron can still hit the conversion dynode, it will be de-

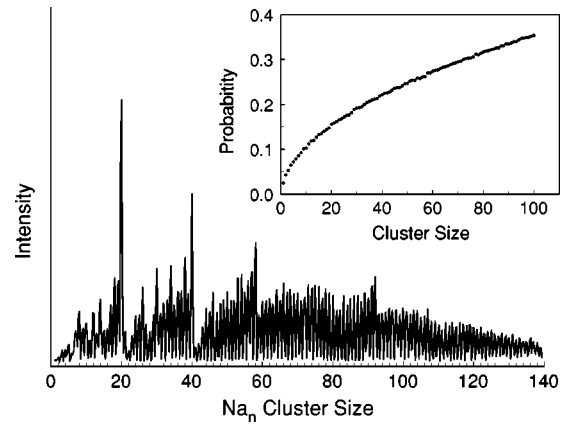


FIG. 2. A mass abundance spectrum recorded during the experiment, displaying the familiar electron shell closings. The insert above the spectrum represents the calculated probability for a negative cluster ion to fly out of the electron gun scattering region and reach the conversion dynode (see text). This probability is less than unity due to the presence of a strong collimating magnetic field inside the electron gun.

tected only if this hit produces a positive secondary particle, a process much less likely for a given impact energy than the ejection of a secondary electron. The end result is a significant reduction in the level of background noise.

The data acquisition mode in our setup can be briefly summarized as follows. The supersonic Na_n beam is mechanically chopped at 94 Hz approximately 50 cm past the source nozzle. After another 1 m of free flight, the clusters enter the scattering region of the electron gun, where some of them form negative ions by capturing low-energy electrons. Since the entire 25-mm-long scattering region is an equipotential volume, the cluster anions leave it with the same translational velocity as the original neutrals in the beam. Elementary ion optics placed behind the scattering region focuses the negatively charged clusters into the Channeltron. The output pulses of the electron multiplier were collected by a plug-in multichannel scaler (MCS) board which was synchronized with the cluster beam chopper. The total counting rate (signal plus noise) was on the order of 3000 counts per second.

For each data point, the nominal electron energy was set and calibrated, the energy distribution (see below) checked, and then a time-resolved MCS profile was accumulated for approximately 25 min. We also monitored the mass population of the original neutral cluster beam by taking mass spectrometer scans before and after each electron energy point. A representative mass spectrum is shown in Fig. 2.

A typical experimental MCS profile is presented in Fig. 3. The scaler starts collecting data immediately after the cluster beam is opened by the chopper wheel. It takes up to 1 ms for the majority of clusters to fly from the chopper to the Channeltron, which accounts for the delay seen before the signal starts to build up above the noise level. From that moment on, the clusters continuously fly through the electron gun until the chopper blocks the beam again. The washed out boundaries of the signal bump are a signature of the intrinsic

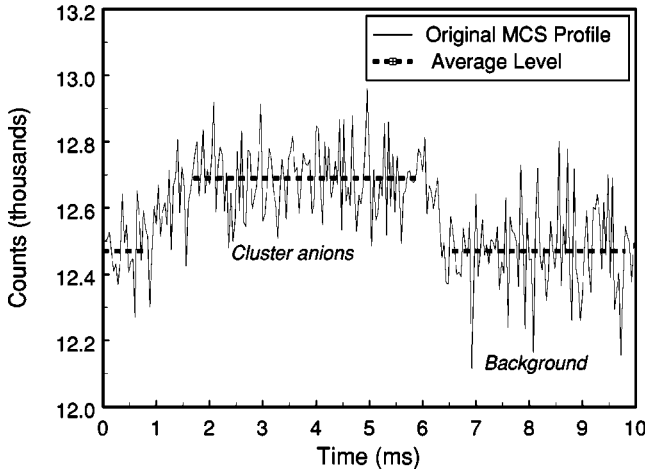


FIG. 3. A typical multichannel scaler profile obtained in our experiment. The chopper wheel opens the cluster beam at time $t = 0$. Following an approximately 1 ms flight time from the chopper, the clusters reach the electron gun and the anion signal builds up above the noise level. After ≈ 5 ms the chopper again gates the beam off. The gradual rise and fall of the cluster signal are a reflection of the intrinsic velocity spread of the beam. The anion current was extracted by summing the counts under the plateau region of the signal “bump” and subtracting the background noise summed over an equivalent number of channels.

cluster velocity spread in the supersonic beam. For every accumulated MCS spectrum, the total amount of real signal, ΔN , was extracted by summing all the channels under the plateau region of the bump and subtracting the noise level for the equivalent number of channels. The estimated accuracy of the extraction is $\sim 10\%$. In this experiment the signal-to-background ratio ranged from $\sim 0.5\%$ to 3% corresponding to a counting rate of up to 10 negative ions per second.

As discussed in detail in our previous publication [26], the following equation relates the effective integral cross section σ_{eff} of the electron-cluster interaction to the measured quantities [36,37]:

$$\frac{\Delta N}{N} = \frac{\sigma_{eff} I_{el}}{v_{cl} h}, \quad (1)$$

where N stands for the neutral cluster flux, I_{el} is the electron number current, h is the height of the interacting beams, and v_{cl} is the cluster beam velocity. Here σ_{eff} is the intrinsic cross section $\sigma(E)$ convoluted with the electron energy distribution $I(E - E_0)$ produced by the electron gun:

$$\sigma_{eff}(E_0) = \frac{\int_0^\infty \sigma(E) I(E - E_0) dE}{\int_0^\infty I(E - E_0) dE}. \quad (2)$$

E_0 represents the nominal electron energy, i.e., the potential applied to the scattering region. A retarding potential technique was used to extract both the electron gun energy spread and the contact potential correction to the nominal

electron energy. The measured energy distribution $I(E - E_0)$ is well represented by a Gaussian shape with a full width at half maximum (FWHM) of about 0.3 eV for $E_0 \leq 1$ eV, and 0.4 eV for higher electron energies. The values for E_0 were measured to an accuracy better than 0.1 eV. For nominal energies less than the FWHM of the electron energy distribution, E_0 is no longer a good measure of the average electron collision energy. In this energy range it is more appropriate to introduce an adjusted electron energy $\langle E \rangle$ as follows [38]:

$$\langle E \rangle = \frac{\int_0^\infty EI(E - E_0) dE}{\int_0^\infty I(E - E_0) dE}, \quad (3)$$

where the energy spread is given an appropriate cutoff at $E = 0$. Note that Eq. 2 for $\sigma_{eff}(E_0)$ truncates $I(E - E_0)$ at the origin as well. Our calculation showed that $\langle E \rangle \approx E_0$ already for nominal energies of 0.5 eV and higher.

As mentioned above, at the moment we do not mass resolve negative ions formed in the electron gun scattering region. This implies that expression (1) should be modified to convolute the mass-dependent σ_{eff} with the mass spectrum produced by the cluster source:

$$\frac{\Delta N}{N} = \left\langle \frac{P \sigma_{eff}}{v_{cl}} \right\rangle \frac{I_{el}}{h} \approx \frac{\langle P \rangle \langle \sigma_{eff} \rangle I_{el}}{\langle v_{cl} \rangle h}. \quad (4)$$

Now N is the *total* number of clusters of all sizes entering the scattering region during the data acquisition cycle, ΔN is the *total* number of detected ions in the same cycle, P is the mass-dependent detection probability for the negative ions in the Channeltron, and the averaging needs to be performed over all the cluster sizes present in the beam. Indeed, in order to be detected the cluster anion should be able first to escape from the scattering region (probability p_1), and then to produce a detected positive fragment (probability p_2) in a collision with the conversion dynode. If we assume that p_1 and p_2 are independent, then $\langle P \rangle = \langle p_1 \rangle \langle p_2 \rangle$. In principle, the probability of the captured electron detaching on the way to the Channeltron should also be addressed. However, such an outcome does not appear to be dominant, and will not be included in our estimates. It is, however, directly related to the fascinating general question of relaxation mechanisms for the negative ions, and as such remains an important subject for future investigation.

A reduced value of p_1 is primarily due to ion deflection by the strong magnetic field B present in the scattering region (the electron beam is collimated by $B = 1400$ G to prevent its dispersal by space charge repulsion [26,39]). Using the equations of charged particle motion in a region of crossed electric and magnetic fields, p_1 can be estimated quite easily and essentially analytically. The inset in Fig. 2 summarizes the variation of cluster escape probability with size. In the mass range of interest, the curve can be very well fitted by a scaled square root function. To find $\langle p_1 \rangle$, the

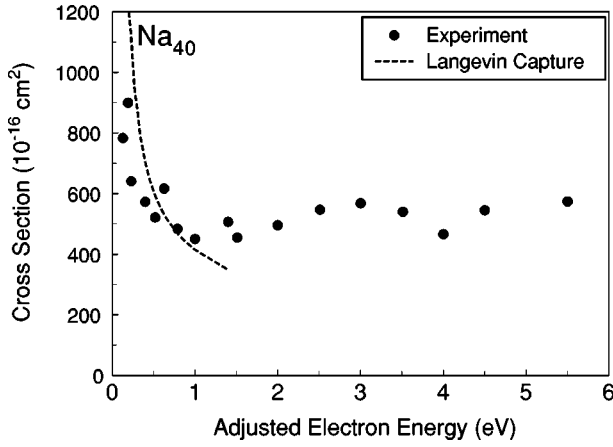


FIG. 4. Total inelastic cross section for collisions of electrons with the closed-shell Na_{40} cluster (from [26]). Solid dots are the experimental data points obtained from a measurement of the relative depletion of the cluster beam. The dashed curve is the Langevin cross section for electron capture by a dipole polarization field, convoluted with the experimental energy resolution. The good quantitative match at low energies was interpreted as evidence for efficient cluster anion formation.

escape probability is convoluted with the mass spectrum distribution measured during the same acquisition cycle [40].

On the other hand, p_2 is expected to be a complicated but relatively level [35] function of the ion mass, its velocity, and the condition of the conversion dynode surface. Thus $\langle p_2 \rangle$ would vary from one data point to another only if the relative intensities of the opposite ends of the mass spectrum showed a strong shift. However, we verified that the “center of gravity” of the mass spectra remained stable to within 10%. Hence it is accurate to treat $\langle p_2 \rangle$ as a constant coefficient. As described in the next section, by scaling the theoretical curve to the experimental data points we estimated $\langle p_2 \rangle \approx 0.03$.

The cluster beam velocity is another parameter entering Eq. (4). In general, in a supersonic beam v_{cl} is a weak function of cluster size. For example, our recent measurements showed [26] that it decreases by less than 10% on going from Na_{20} to Na_{70} . Thus we used an average value $\langle v_{cl} \rangle = 1100$ m/s in the expression (4) instead of performing velocity measurements for every cluster in the mass spectrum.

III. RESULTS

As described in the Introduction, this experiment was carried out in order to verify directly that cluster beam depletion as a result of collisions with 0–1 eV electrons is primarily due to negative cluster ion formation [25,26].

For reference, Fig. 4 shows the previously measured total inelastic electron scattering cross section for Na_{40} as a function of the collision energy. The dots are the experimental data points extracted from the depletion of the cluster beam in accordance with Eq. (1). The dashed line represents the Langevin electron capture cross section

$$\sigma_{cap}(E) = \sqrt{\frac{2\pi^2 e^2 \alpha}{E}}, \quad (5)$$

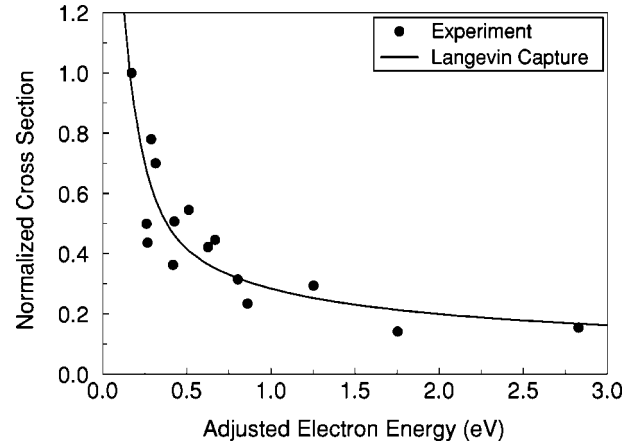


FIG. 5. The main result of this work: direct evidence for negative-ion formation in collisions of low-energy electrons with neutral sodium clusters Na_n . Circles: anion yield normalized to the neutral cluster flux and to the electron current. Line: Langevin electron capture cross section convoluted with the mass abundance spectrum and with the electron gun resolution (see text). The only adjustable parameter is an overall scaling factor representing primarily the Channeltron detection efficiency. It is concluded that ion formation proceeds via electron capture by the polarization field of the cluster.

where E is the energy of the incoming electron and α is the cluster polarizability. As mentioned in Sec. I, this cross section represents an electron trajectory spiraling into the cluster center under the influence of the polarization potential $V_{pol} = -\alpha e^2/2r^4$. The plateau section ($E > 1$ eV) of the depletion curve in Fig. 4 was interpreted as the onset of electron-induced cluster fragmentation.

The results of our present direct measurement of anion formation are shown in Fig. 5. The experimental data points are normalized to a value of 1 for the maximum cross section in the set (absolute scaling is hampered primarily by the absence of quantitative information on the dynode conversion probability $\langle p_2 \rangle$ defined in Sec. II). Since it enters expression (4) as an overall scaling factor, the normalization obviously does not affect the intrinsic energy dependence of the measured ion yield. The relative accuracy of the data points shown in Fig. 5 is estimated to be 10–15%.

The Langevin capture cross section (5) depends on the cluster size n through the polarizability α . Obviously, different cluster sizes will have different numerators in the Langevin formula. But the energy denominator remains the same for all particles. Hence, if the electron capture mechanism is relevant to our case, the overall shape should follow an inverse square root dependence on the collision energy:

$$\langle \sigma_{cap}(E) \rangle = \sum_n f(n) \sigma_{cap}(E, n) = \frac{A}{\sqrt{E}}. \quad (6)$$

Here $f(n)$ is the relative abundance of Na_n in the beam, and A is the resulting overall numerator.

The solid line in Fig. 5 is a least-squares fit of the const/\sqrt{E} dependence to the set of experimental anion yield data. This function was convoluted with the electron gun

energy resolution prior to fitting, as defined in Eq. (2). There is an impressively good agreement between the shape of the curve and the experimental points. This result directly confirms that the observed cross section rise for $E \rightarrow 0$ is a signature of electron capture.

Electron attachment processes may be affected by resonances, thresholds, Franck-Condon factors, etc. It would be very interesting and challenging to search for such features in a high-resolution measurement. Our data, which are focused on the general energy dependence of the cross section, indicate that the polarization interaction is the controlling factor: its long range dominates over the contribution of other phenomena.

Finally, let us estimate the average probability $\langle p_2 \rangle$ for cluster anion conversion into positive fragments at the conversion dynode. This can be found from Eq. (4) by substituting into it the relevant electron and cluster beam parameters and intensities, together with Eq. (6) for the averaged capture cross section. The numerator A in the latter is given, according to Eq. (5), by

$$A = \pi e \sum_n f(n) \sqrt{2\alpha_n}. \quad (7)$$

To perform the averaging over the cluster mass spectrum, we need to know how the polarizability of a cluster depends on its size n . For alkali-metal clusters, it can be adequately fitted by the form $\alpha_n = (R_n + \delta)^3$, where $R_n = r_s a_0 n^{1/3}$ is the cluster core radius ($r_s = 3.96$ is the Wigner-Seitz parameter for sodium and a_0 is the Bohr radius) and $\delta \approx 0.75 \text{ \AA}$ is the valence electron spill-out parameter [23]. Using Eq. (7), together with an estimate that the detection efficiency of the supersonic beam by the mass spectrometer unit is 30%, we found that the average conversion dynode probability $\langle p_2 \rangle$ is approximately equal to 0.03: on average only 3% of cluster anions incident on the dynode are detected by the CEM. This is, indeed, a realistic value [35].

IV. DISCUSSION AND SUMMARY

In summary, we have studied the interaction of a beam of low-energy electrons with free neutral sodium clusters. We have directly observed efficient formation of negatively charged Na_n^- ions in the 0–3 eV collision energy range,

confirming an earlier conjecture. The energy dependence of the experimental anion yield is in excellent agreement with the Langevin mechanism of electron capture in the cluster polarization potential.

This result raises further important experimental and theoretical questions regarding the mechanisms of negative-ion formation and relaxation. In the molecular case, attachment often goes through an intermediate resonant excited state [2–4] which subsequently decays via a variety of channels. It is an interesting question whether a similar intermediate state is formed in electron–metal–cluster collisions (and what its lifetime is), or whether the electron “falls into the cluster” directly, with its energy redistributed into the vibrational, collective, or particle-hole excitations of the latter [41–43], or lost by radiation [44,45]. A related question concerns the stability of the freshly formed cluster anions: do they undergo fast direct fragmentation (“dissociative attachment” [11,46]), heat up and evaporate (“evaporative attachment” [12]), or are they relatively long lived? It is probable that the answer is sensitive to the cluster size and the collision energy, and therefore encompasses a variety of dynamical processes. These issues will be addressed in further work; in particular, the first aim will be to achieve mass selectivity of the cluster anions formed in the electron gun.

It should also be noted that the Langevin formula (5) has been derived in the electric dipole approximation. What would happen if terms higher than $1/r^4$ were included in the polarization potential? The corresponding classical capture cross section can be calculated exactly, and we find that for the cluster sizes studied in this experiment ($n \lesssim 10^2$) the correction to the Langevin cross section is minor. However, for larger sizes (over 1000 atoms per cluster), the electric dipole approximation is found to be insufficient, and the full image charge potential needs to be invoked to explain the experimental results [47].

ACKNOWLEDGMENTS

We would like to thank Jay Ray and Laura Ray of De-Tech and Rick Schaeffer of ABB Extrel for valuable technical advice, and the staff of the USC Natural Science Machine Shop for expert machining. This work was supported by the U.S. National Science Foundation under Grant No. PHY-9600039.

-
- [1] M.K. Scheller, R.N. Compton, and L.S. Cederbaum, *Science* **270**, 1160 (1995).
 - [2] A. Chutjian, A. Garscadden, and J.M. Wadehra, *Phys. Rep.* **264**, 6 (1996).
 - [3] O. Ingólfsson, F. Weik, and E. Illenberger, *Int. J. Mass Spectrom. Ion Processes* **155**, 1 (1996).
 - [4] E. Illenberger and B.M. Smirnov, *Usp. Fiz. Nauk* **168**, 731 (1998) [*Phys. Usp.* **41**, 651 (1998)].
 - [5] B. Boudaïffa, P. Cloutier, D. Hunting, M.A. Huels, and L. Sanche, *Science* **287**, 1658 (2000).
 - [6] R.G. Keesee, A.W. Castleman, Jr., and T.D. Märk, in *Swarm Studies and Inelastic Electron-Molecule Collisions*, edited by L.C. Pitchford, B.V. McCoy, A. Chutjian, and S. Trajmar (Springer, New York, 1987).
 - [7] A.S. Stamatović and T.D. Maerk, *Rapid Commun. Mass Spectrom.* **5**, 51 (1991).
 - [8] H.S. Carman, Jr., *J. Chem. Phys.* **100**, 2629 (1994).
 - [9] S. Matejcik, P. Stampfli, A. Stamatovic, P. Scheier, and T.D. Märk, *J. Chem. Phys.* **111**, 3548 (1999).
 - [10] G. Senn, D. Muigg, G. Denifl, A. Stamatovic, P. Scheier, and

- T.D. Märk, *Eur. Phys. J. D* **9**, 159 (1999).
- [11] J.M. Weber, E. Leber, M.-W. Ruf, and H. Hotop, *Phys. Rev. Lett.* **82**, 516 (1999).
- [12] J.M. Weber, E. Leber, M.-W. Ruf, and H. Hotop, *Eur. Phys. J. D* **7**, 587 (1999).
- [13] S. Matejcik, T.D. Märk, P. Spänel, D. Smith, T. Jaffke, and E. Illenberger, *J. Chem. Phys.* **102**, 2516 (1995).
- [14] J. Huang, H.S. Carman, Jr., and R.N. Compton, *J. Phys. Chem.* **99**, 1719 (1995).
- [15] D. Smith and P. Spänel, *J. Phys. B* **29**, 5199 (1996).
- [16] J.M. Weber, M.-W. Ruf, and H. Hotop, *Z. Phys. D* **37**, 351 (1996).
- [17] O. Elhamidi, J. Pommier, and R. Abouaf, *J. Phys. B* **30**, 4633 (1997).
- [18] A. Vostrikov, D. Yu. Dubov, and A.A. Agarkov, *Pis'ma Zh. Tech. Fiz.* **21**, 55 (1995) [*Tech. Phys. Lett.* **21**, 517 (1995)].
- [19] L. Schweikhard, A. Herlert, S. Krückeberg, M. Vogel, and C. Walther, *Philos. Mag. B* **79**, 1343 (1999).
- [20] W.D. Knight, K. Clemenger, W.A. de Heer, and W.A. Saunders, *Phys. Rev. B* **31**, 2539 (1985).
- [21] E. Benichou, R. Antoine, D. Rayane, B. Vezin, F.W. Dalby, Ph. Dugourd, M. Broyer, C. Ristori, F. Chandezon, B.A. Huber, J.C. Rocco, S.A. Blundell, and C. Guet, *Phys. Rev. A* **59**, R1 (1999).
- [22] D. Rayane, A. Allouche, E. Benichou, R. Antoine, M. Aubert-Frecon, Ph. Dugourd, M. Broyer, C. Ristori, F. Chandezon, B.A. Huber, and C. Guet, *Eur. Phys. J. D* **9**, 243 (1999).
- [23] K.D. Bonin and V.V. Kresin, *Electric-Dipole Polarizabilities of Atoms, Molecules and Clusters* (World Scientific, Singapore, 1997).
- [24] V.V. Kresin and C. Guet, *Philos. Mag. B* **79**, 1401 (1999).
- [25] V.V. Kresin, A. Scheidemann, and W.D. Knight, in *Electron Collisions with Molecules, Clusters, and Surfaces*, edited by H. Ehrhardt and L.A. Morgan (Plenum, New York, 1994).
- [26] V. Kasperovich, G. Tikhonov, K. Wong, P. Brockhaus, and V.V. Kresin, *Phys. Rev. A* **60**, 3071 (1999).
- [27] P. Langevin, *Ann. Chim. Phys.* **5**, 245 (1905).
- [28] L.D. Landau and E.M. Lifshitz, *Mechanics*, 3rd ed. (Pergamon, Oxford, 1976), Sec. 18.
- [29] E.W. McDaniel, *Atomic Collisions: Electron and Photon Projectiles* (Wiley, New York, 1989).
- [30] E. Vogt and G.H. Wannier, *Phys. Rev.* **95**, 1190 (1954).
- [31] E.A. Kurz, *Am. Lab.* **11**, 67 (1979).
- [32] Galileo Electro-Optics Corporation, "Channeltron Electron Multiplier Handbook for Mass Spectrometry Applications" (Sturbridge, MA, 1991).
- [33] H. Haberland and M. Winterer, *Rev. Sci. Instrum.* **54**, 764 (1983).
- [34] P.G. Friedman, K.J. Bertsche, M.C. Michel, D.E. Morris, R.A. Muller, and P.P. Tans, *Rev. Sci. Instrum.* **59**, 98 (1988).
- [35] G.C. Stafford, *Environ. Health Perspect.* **36**, 85 (1980).
- [36] B. Bederson and L.J. Kieffer, *Rev. Mod. Phys.* **43**, 601 (1971).
- [37] R.E. Collins, B. Bederson, and M. Goldstein, *Phys. Rev. A* **3**, 1976 (1971).
- [38] A.A. Agarkov, V.A. Galichin, S.V. Drozdov, D.Yu. Dubov, and A.A. Vostrikov (unpublished).
- [39] It is a beneficial property of the Channeltron detector that its normal operation is not impaired by magnetic fields of up to 1 T (B. Lincoln, Galileo Electro-Optics Corporation, private communication).
- [40] Strictly speaking, the mass spectrum shown in Fig. 2 displays the relative abundances of positive clusters ionized in the beam detector, and not of the neutral ones passing through the electron gun. However, there is much evidence that soft filtered UV light can ionize the clusters with minimal heating and without significant fragmentation [see, e.g., K. Selby, M. Vollmer, J. Masui, V. Kresin, W.A. de Heer, and W.D. Knight, *Phys. Rev. B* **40**, 5417 (1989); S. Björnholm and J. Borggreen, *Philos. Mag. B* **79**, 1321 (1999)]. Hence averaging over the detected mass spectrum is adequate for a calculation of $\langle p_1 \rangle$, especially considering that the escape probability shown in the inset is a smooth function of cluster size and would not be significantly affected by a small shift in n .
- [41] M.R. Spinella, M. Bernath, O. Dragún, and H. Massmann, *Phys. Rev. A* **54**, 2197 (1996).
- [42] L.G. Gerchikov, A.V. Solov'yov, J.-P. Connerade, and W. Greiner, *J. Phys. B* **30**, 4133 (1997).
- [43] L.G. Gerchikov, A.N. Ipatov, and A.V. Solov'yov, *J. Phys. B* **30**, 5939 (1997).
- [44] J.P. Connerade and A.V. Solov'yov, *J. Phys. B* **29**, 365 (1996).
- [45] M.R. Spinella, M. Bernath, and O. Dragún, *Phys. Rev. A* **58**, 2985 (1998).
- [46] M. Keil, T. Kolling, K. Bergmann, and W. Meyer, *Eur. Phys. J. D* **7**, 55 (1999).
- [47] V. Kasperovich, K. Wong, G. Tikhonov, and V.V. Kresin, *Phys. Rev. Lett.* **85**, 2729 (2000).